N. Hiroshiba

About this author version (hiroshiba@bunko2.bk.tsukuba.ac.jp)

Nobuya Hiroshiba, *et al.*, *Thin Solid Films*, **518** (2), 441-443, 2009
http://dx.doi.org/10.1016/j.tsf.2009.07.050

Title: Structural analysis and transistor properties of hetero-molecular bilayers

Author: Nobuya Hiroshiba[1, 2], Ryoma Hayakawa[1], Matthieu Petit[1], Toyohiro Chikyow[1], Kiyoto Matsuishi[2], Yutaka Wakayama[1, (a)]

[1]Advanced Electronic Materials Center, National Institute for Materials Science, 1-1 Namiki, Tsukuba, 305-0044, Japan

[2]Graduate School of Pure and Applied Science, University of Tsukuba, 1-1-1 Tennoudai, Tsukuba, 305-8571, Japan

[(a)] Corresponding author: WAKAYAMA.Yutaka@nims.go.jp

TEL: +81-29-860-4403 / FAX: +81-29-860-4916

Nobuya Hiroshiba, *et al.*, *Thin Solid Films*, **518** (2), 441-443, 2009
http://dx.doi.org/10.1016/j.tsf.2009.07.050

ABSTRACT

We examined the film morphologies and transistor properties of hetero-molecular bilayer consisting of *N, N'*-dioctyl-3, 4, 9, 10- perylenedicarboximide (PTCDI-C_8) and quaterrylene. First, the structure and carrier conduction of PTCDI-C_8 films were studied, followed by an analysis of the carrier accumulation process in a PTCDI-C_8/quaterrylene hetero-bilayer transistor. Based on the displacement current measurement (DCM), we stress the potential of the hetero-bilayer for tuning carrier accumulation like carrier doping techniques in field-effect transistors.

Nobuya Hiroshiba, *et al.*, *Thin Solid Films*, **518** (2), 441-443, 2009
http://dx.doi.org/10.1016/j.tsf.2009.07.050

INTRODUCTION

The main purpose of this study is to describe the structural and electrical characteristics of binary molecular layers. Particular emphasis is placed on carrier trapping at a hetero-molecular interface.

Various organic devices have attracted attention owing to their excellent potential. A typical example is the organic field-effect transistor (OFET), which is designed for use as an information processing unit such as a radio frequency tag. Recent studies have indicated the significance of hetero-material interfaces. Well-defined interfaces, such as the bulk hetero-junctions in organic photovoltaic (OPV) cells [1], multi-photon emission structures in organic light emitting diodes (OLEDs) [2] and modified hetero-interfaces in OFETs [3, 4], have improved the performance of organic devices. However, with only a few successful exceptions, interface engineering has yet to be fully applied to OFETs [4]. Highly controlled hetero-interfaces at the single layer level are essential for OFETs because the thickness of the carrier accumulation layer is limited to the first few monolayers in OFETs [5]. The early stage of molecular layer growth has been studied using scanning tunneling microscopy, photoelectron spectroscopy and the Kelvin Probe method [6-8]. By contrast, few studies have reported the relationships between film structures at the monolayer level or OFET properties.

Nobuya Hiroshiba, *et al.*, *Thin Solid Films*, **518** (2), 441-443, 2009
http://dx.doi.org/10.1016/j.tsf.2009.07.050

In this study, we report a structural analysis and the transistor properties of hetero-molecular bilayers to determine the possibilities of novel functionalities such as the quantum confinement effect, charge transfer and optical carrier doping in organic devices. We used the ultra slow deposition technique [9-11], which enabled us to achieve layer-by-layer growth and to evaluate the OFET accumulation layer at a monolayer level. In our experiments we employed PTCDI-C_8 and quaterrylene molecules, which exhibit n- and p-type performance, respectively [12, 13]. First, we provide an analysis of the morphology and molecular orientation of PTCDI-C_8 layers. Then, we examine the morphology and molecular orientation of PTCDI-C_8/quaterrylene binary layers to investigate the effect of an organic-organic interface on carrier transfer and trapping.

Nobuya Hiroshiba, *et al.*, *Thin Solid Films*, **518** (2), 441-443, 2009
http://dx.doi.org/10.1016/j.tsf.2009.07.050

EXPERIMENTAL

PTCDI-C_8 molecules (Fig. 1 (a)) were deposited on SiO_2/Si substrates using an ultraslow deposition technique [9, 10] in a high vacuum (~10^{-6} Pa). The deposition rate was less than 0.03 monolayers (ML) per minute. The substrate temperature was optimized at 140 ^{o}C. The films thus prepared were investigated using the x-ray reflection (XRR) technique (Bruker AXS: D8 Discover, Cu-Kα; λ=0.154 nm), which is a useful method for estimating the thickness and roughness of multi layer structures with 0.1 nm accuracy [14, 15], and atomic force microscopy (AFM) in a dynamic force mode (Seiko Instruments Inc, SPI-4000 E-sweep).

All the processes including the preparation and electrical measurement of the OFETs were carried out in a vacuum without exposure to the air. The OFETs of a PTCDI-C8 single component with top-contact Al electrodes prepared in a deposition chamber were transferred into a semiconductor device analyzer (Agilent, B1500A) by a vacuum transfer system. After transistor analysis at room temperature, quaterrylene molecules were deposited on top of the PTCDI-C_8 FETs. Subsequently, the transistor properties of the PTCDI-C_8/quaterrylene hetero-bilayer were compared before and after quaterrylene deposition. Displacement current measurement (DCM) [16, 17] was used to confirm the carrier injection process. The DCM method enables us to examine the

carrier injection process and to estimate the number of injected carriers. In our setup, the drain current was monitored at a DCM sweep speed of 1 V/sec.

Nobuya Hiroshiba, *et al.*, *Thin Solid Films*, **518** (2), 441-443, 2009
http://dx.doi.org/10.1016/j.tsf.2009.07.050

RESULTS AND DISCUSSION

Figure 2(a) shows an AFM image of PTCDI-C_8 with a 2.3 ML thickness. Flat terraces and clear step edges provide evidence of layer-by-layer growth. PTCDI-C8 films with different thicknesses (0.8, 1.1 and 2.3 ML) were prepared for the FET measurements. Normally off n-type operations were observed only from the 2.3 ML transistor as shown in Fig. 2(b) and (c). The on-off ratio and threshold voltage were 2 x 10^3 and -0.7 V, respectively (Fig. 2(c)). Meanwhile, no transistor operation was observed in the 0.8 and 1.1 ML FETs. We assumed that there was a thermal effect that occurred during the deposition of the molecular layer and/or that the Al electrodes affected the molecular orientation in the first few layers. To analyze the absence of transistor operation and to confirm our assumption, we investigated the molecular orientation using XRR.

Figure 3(a) shows XRR spectra obtained from an as-deposited PTCDI-C_8 monolayer (upper plot), a thermally treated momolayer (middle plot) and an as-deposited 2.3 ML (lower plot). The thermal treatment was performed at 160 ^oC for 3 hours after deposition. The XRR spectra clearly reveal distinct differences in molecular orientation. The thicknesses were estimated to be 2.8 and 1.2 nm for the as-deposited and thermally treated monolayers, respectively, and 4.2 nm for the as-deposited 2.3 ML.

It is reasonable to consider that the PTCDI-C_8 molecules have an upright orientation to the SiO_2 surface normal as shown in the upper illustration in Fig. 3(a). In contrast, the thickness of 1.2 nm after thermal treatment indicates that the first layer of PTCDI-C_8 molecules lie on the substrate (middle illustration in Fig. 3(a)), suggesting that the first PTCDI-C_8 layer is easily affected by temperature. As a result, the first PTCDI-C_8 layer is unable to perform as a continuous channel layer (Fig. 3(b)). The result for the 4.2 nm thick 2.3 ML indicates that the first layer lies down during the subsequent deposition, followed by the second layer with an upright orientation. Consequently, only the second layer can act as a conduction path as shown in Fig. 3(c).

To examine the effects of the hetero-molecular interface, 1.5 ML of quaterrylene, which functions as a p-type semiconductor, was deposited on top of the PTCDI-C_8 2.3 ML transistor. Figure 4(a) shows an I_D-V_G curve for a hetero-bilayer transistor (blue dots). Here, the curve for the PTCDI-C_8 transistor (red dots) from Fig. 2(c) is shown for comparison. The hetero-bilayer transistor exhibited only n-type operation at gate voltages of -60 to 60 V. The threshold voltage was estimated to be 1.2 V. An increase in the off-current and a decrease in the on-current were observed. As a result, the on-off ratio of the hetero-OFET was 2 x 10, which is 10^{-2} times lower than that of the PTCDI-C8 FET.

Nobuya Hiroshiba, *et al.*, *Thin Solid Films*, **518** (2), 441-443, 2009
http://dx.doi.org/10.1016/j.tsf.2009.07.050

First, AFM observation was carried out to explain these experimental results. Figure 4(b) shows the surface morphology of the hetero-bilayer, revealing that the quaterrylene formed 3-dimensional islands. Thus, quaterrylene molecules did not form a carrier transport path as illustrated in the inset of Fig. 4 (b). This explains the absence of p-type operation. Hence, we can conclude that the carrier transport observed in Fig. 4(a) originates from the PTCDI-C_8 layer and the changes in the on- and off-currents can be attributed to the influence of the PTCDI-C_8/quaterrylene interface.

We employed the DCM method to gain a further understanding of the effect of the PTCDI-C_8/quaterrylene interface on the V_{th} shift and on-off currents. The DCM spectra of the PTCDI-C_8 and hetero-bilayer transistors are shown in Fig. 4 (c). The peak of the PTCDI-C_8 FET observed around V_G= 5 V split into two peaks (V_G=-5 and 20 V) after the deposition of the quaterrylene layer. The peak observed at V_G=-5 V indicates that carrier injection occurred at this voltage. However, there was no increase in the source-drain current (I_D) at V_G= -5 V in the I_D-V_G curve of the hetero-FET (Fig. 4(a)). Therefore, the peak at V_G=-5 V reveals that a new energy state was formed by quaterrylene deposition and did not contribute to carrier conduction. In addition to this result, the peak observed at V_G=20 V can be identified as the shifted peak of the PTCDI-C_8 FET originally observed at V_G =5 V. In consequence, the carriers were first

injected into the interface state created at PTCDI-C_8/quaterrylene interface, thus causing V_{th} to shift to a higher voltage (Fig. 4(d)). As a result, the accumulated carriers in the PTCDI-C_8 layer decreased. This explains the on-current decrease observed in Fig. 4(a). In addition, the carriers trapped at the PTCDI-C_8/quaterrylene interface can be thermally activated thus increasing the off-current.

In summary, we discussed the film structure and transistor properties of a PTCDI-C_8/quaterrylene hetero-bilayer. AFM and XRR analyses clarified the film morphology and molecular orientation. The DCM results clarify the carrier injection and accumulation processes in the hetero-bilayer transistor. Particular emphasis was placed on the interface state created at the hetero-molecule interface, which caused a shift in V_{th} and changes in the on-off currents. These results suggest the potential of the hetero-molecular interface for tuning carrier concentration and dynamics; an appropriate choice of molecule combination, such as a HOMO-LUMO level arrangement, will enable us to achieve the fine control of carriers like conventional Si devices.

Nobuya Hiroshiba, *et al.*, *Thin Solid Films*, **518** (2), 441-443, 2009
http://dx.doi.org/10.1016/j.tsf.2009.07.050

REFERENCE

[1] Pavel Schilinsky, Christoph Waldauf, Christoph J. Brabec, *Appl. Phys. Lett*., **81**, 3885 - 3887, 2002

[2] Junji Kido, Toshio Matsumoto, Takeshi Nakada, Jun Endo, Kohichi Mori, Norifumi Kawamura, and Akira Yokoi, *SID Symposium Digest of Technical Papers*, **34**, 964 - 965, 2003

[3] Nobuya Hiroshiba, Katsumi Tanigaki, Ryotaro Kumashiro, Hirotaka Ohashi, Takatsugu Wakahara and Takeshi Akasaka, *Chem. Phys. Lett*. **400**, 235 - 238, 2004

[4] S. Kobayashi, T. Nishikawa, T. Takenobu, S. Mori, T. Shimoda, T. Mitani, H. Shimotani, N. Yoshimoto, S. Ogawa, Y. Iwasa, *Nature Materials* **3**, 317, 2004

[5] K. Marumoto, Shin-ichi Kuroda, Taishi Takenobu, and Yoshihiro Iwasa, *Phys. Rev. Lett*., **97**, 256603, 2006

[6] Yutaka Wakayama, Jonathan P. Hill and Katsuhiko Ariga, *Surface Science*, **601**, 3984-3987, 2007

[7] Hisao Ishii, Kiyoshi Sugiyama, Eisuke Ito, Kazuhiko Seki, Advanced materials, **11**, 605 - 625, 1999

[8] Nobuo Ueno, Satoshi Kera, Kazuyuki Sakamoto, Koji K. Okudaira, Appl. Phys. A, **92**, 495-504, 2008

[9] H. Sasaki, Y. Wakayama, T. Chikyow, E. Barrena, H. Dosch and K. Kobayashi Appl. Phys. Lett. **88**, 081907, 2006

[10] R. Hayakawa, M. Petit, Y. Wakayama and T. Chikyow, *Organic Electronics,* **8,** 631-634, 2007

[11] Matthieu Petit, Ryoma Hayakawa, Yutaka Wakayama, and Toyohiro Chikyow, *Journal of Physical Chemistry C,* **111,** 12747 – 12751, 2007

[12] Würthner, F. *Chem. Commun.,* **2004**, *14*, 1564

[13] Reid J. Chesterfield, John C. McKeen, Christopher R. Newman, Paul C. Ewbank, Deme´trio A. da Silva Filho, Jean-Luc Bre´das, Larry L. Miller, Kent R. Mann, C. Daniel Frisbie, *J. Phys. Chem. B,* **108**, 19281-19292, 2004

[14] V.Holy, J.Kubena and I.Ohlidal, K.Lischka, W.Plotz, Phys. Rev. B., **47,** 15896 1993

[15] XRR simulations and fitting were calculated by DIFFRAC^{plus} *LEPTOS* (Bruker AXS Inc., XRR analysis software).

[16] S. Egusa, A. Miura, N. Gemma, A. Miura and M. Azuma, *Jpn. J. Appl. Phys.* **33**, 2741, 1994

[17] S. Ogawa, Y. Kimura, H. Ishii and M. Niwano, *Jpn. J. Appl. Phys* **42**, L 1275, 2003

FIGURE CAPTIONS

Figure 1(a) Chemical formula of PTCDI-C8 molecules and its space-filling model and lengths. (b) Chemical formula of quaterrylene molecules and its model

Figure 2(a) AFM images of 2.3 ML surface (b) typical I_D-V_D characteristics of a PTCDI-C8 FET and (c) I_D-V_G characteristics measured in the saturation region.

Figure 3(a) XRR results for as-deposited PTCDI-C8 first layer (upper plot), PTCDI-C8 first layer after thermal treatment (middle plot) and as-deposited 2.3 ML layer of PTCDI-C8 (lower plot). (b) Model illustration of first PTCDI-C8 layer and (c) first and second bilayers of PTCDI-C8.

Figure 4(a) I_D-V_G characteristics of hetero-bilayer FET, (b) AFM images of hetero-bilayer transistor and (inset) illustration of hetero-OFET (c) DCM results for full-range measurements (inset) and first increasing sweep step of PTCDI-C8 FET and hetero-bilayer FET (d) schematic energy diagram of PTCDI-C8 and hetero-bilayer FETs.

Nobuya Hiroshiba, *et al.*, *Thin Solid Films*, **518** (2), 441-443, 2009
http://dx.doi.org/10.1016/j.tsf.2009.07.050

Figure 1

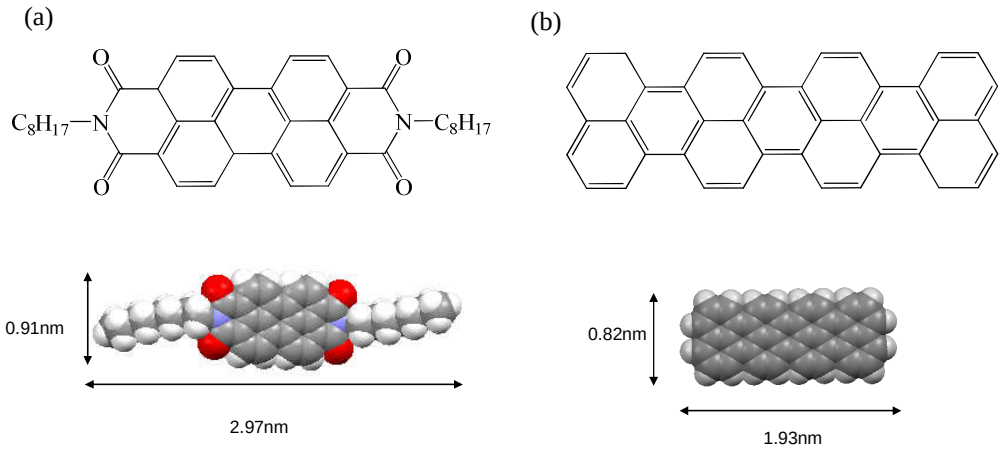

Figure 2

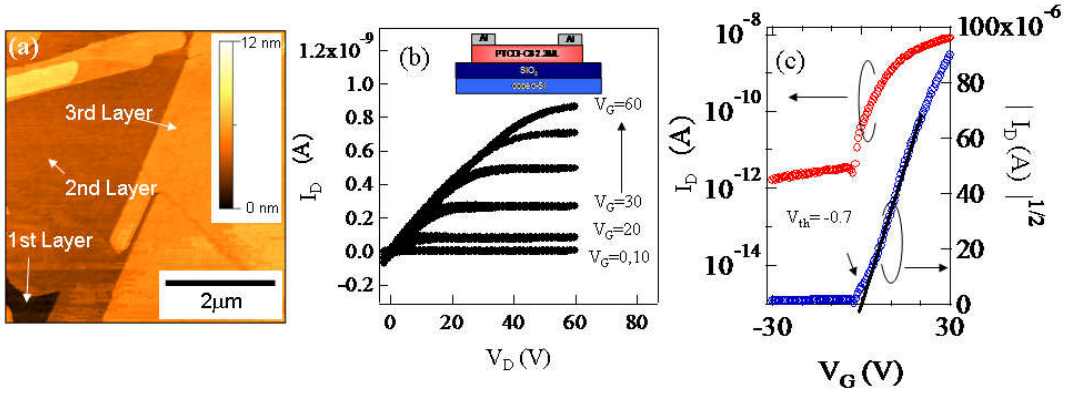

Nobuya Hiroshiba, *et al.*, *Thin Solid Films*, **518** (2), 441-443, 2009
http://dx.doi.org/10.1016/j.tsf.2009.07.050

Figure 3

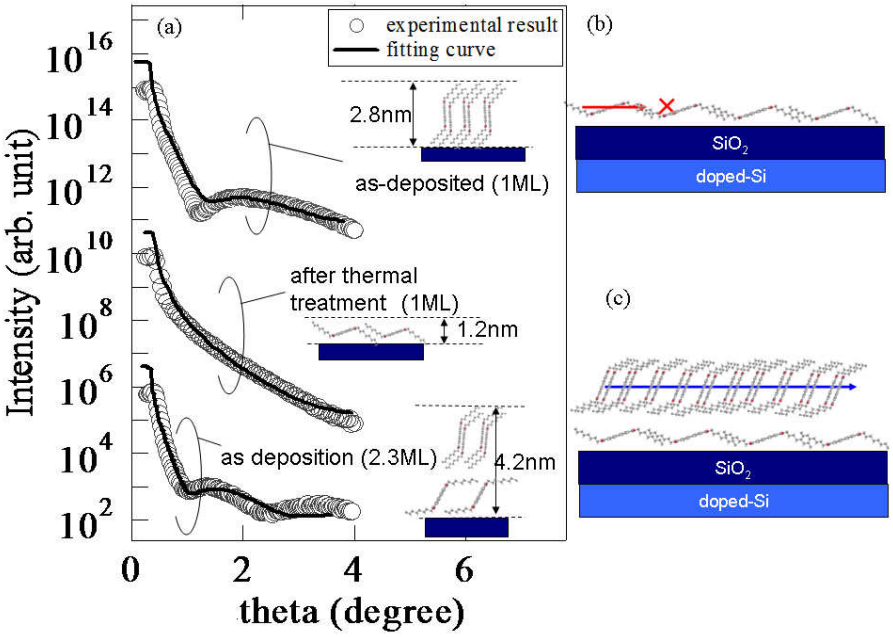

Figure 4

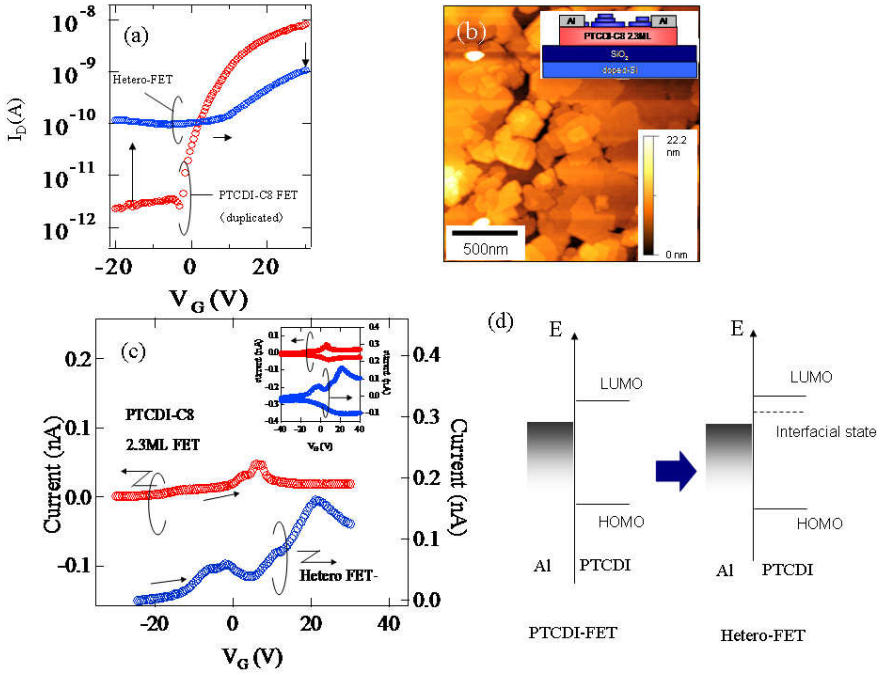

Nobuya Hiroshiba, *et al.*, *Thin Solid Films*, **518** (2), 441-443, 2009
http://dx.doi.org/10.1016/j.tsf.2009.07.050